Front. Earth Sci. 2023, 17(3): 661−678
https://doi.org/10.1007/s11707-022-1063-5

RESEARCH ARTICLE

Geochemical characteristics of produced fluids from CBM wells and their indicative significance for gas accumulation in Daning-Jixian block, Ordos Basin

Taotao YAN (✉)[1,2], Chao YANG[2], Shuai ZHENG[3], Yadong BAI[4], Wei CHEN[5], Yanfei LIU (✉)[1], Wenguang TIAN[6], Shasha SUN[6], Shangwen JIN[1], Jiahang WANG[7], Zhenxing LIU[8], Huifang YAO[1]

1 College of Mining Engineering, Taiyuan University of Technology, Taiyuan 030024, China
2 Coal Reservoir Laboratory of National Engineering Research Center of CBM Development & Utilization, China University of Geosciences, Beijing 100083, China
3 China Coal Geology Group Co., Ltd, Beijing 100043, China
4 Research Institute of Petroleum Exploration and Development (Northwest), PetroChina, Lanzhou 730000, China
5 Beijing Furuibao Energy Technology Company, Beijing 100176, China
6 PetroChina Research Institute of Petroleum Exploration and Development, Beijing 100083, China
7 Engineering Institute of SINOPEC Shanghai Offshore Oil & Gas Company, Shanghai 200120, China
8 Exploration and Development Research Institute of PetroChina Huabei Oilfield Company, PetroChina, Renqiu 062552, China

© Higher Education Press 2023

Abstract The Daning-Jixian block, the eastern edge of the Ordos Basin, is one of the most potential areas for CO_2 geological storage, enhanced coalbed methane recovery (ECBM) exploration and production in China in recent decades. The ionic composition and total dissolved solids (TDS) of the produced water, coal organic matter maturity, molecular composition and carbon isotope characteristics of the produced gas were utilized to analyze the hydrogeological condition, CBM generation and migration characteristics in this area. The CBM enrichment patterns and the geological impacts on gas well production characteristics were revealed. The optimal area for CBM development and CO_2 geological storage in the study area were also proposed. Dominated by the Xueguan reverse fault zone, the hydraulic unit in this area can be divided into two parts (i.e., the recharge-runoff zone in the east and the weak runoff-stagnation zone in the west). The thermogenic gas is dominating CBM genesis in this area. Secondary biogenic gas replenishment is only distributed in the eastern margin area, where the $\delta^{13}C_1$ value is less than the thermal simulation results as an influence of hydrodynamic fractionation. Finally, two models of CBM formation and accumulation were proposed, 1) thermogenic CBM migrated by hydrodynamic and resorbed for preservation at impermeable fault boundaries; 2) thermogenic CBM trapped by fault and accumulated by hydrodynamic in slope zone. The gas production performance, generally increased from east to west, is mainly dominated by hydrogeological conditions. Generally, the west side of the fault zone is the enrichment and high-yield area for ECBM development and CO_2 geological storage in the study area.

Keywords produced water and gas, gas accumulation, geochemical parameter, CBM production, CO_2 geological storage, Daning-Jixian block

Received August 31, 2022; accepted November 14, 2022

E-mail: taotao87225@163.com (Taotao YAN)
liuyanfei@tyut.edu.cn (Yanfei LIU)

1 Introduction

The Ordos Basin is endowed with abundant coal, oil and gas resources, which is an important area for fossil fuel exploration and development and CO_2 geological storage in China. The Daning-Jixian block is the southern part of the Jinxi flexural zone in the eastern margin of Ordos Basin (Fig. 1), which has shown a great potential for CBM exploitation and CO_2 geological storage, with a total gas-bearing area of up to 1419 km^2 (Sun et al., 2004) and a predicted CBM resource of about 0.6 × 10^8 m^3. In recent years, many research works have been carried out in the Daning-Jixian block. Sun and Wang (2006) analyzed the sedimentary environment of C-P coal-bearing strata in this area. Yang (2003) evaluated the physical properties of coal reservoir and predicted the high permeability area of the Daning-Jixian block. Jiang et al. (2016) analyzed the current stress field distribution by using logging data in this area. Chao and Wang (2016) discussed the genetic types and hydrodynamic conditions of CBM in this block. Zhang et al. (2022) analyzed the relationship between trace elements in produced water and production characteristics. However, there is a lack of systematic research on the geological influences on the enrichment, accumulation, production of CBM and potential areas prediction for CO_2 geological storage in this area.

The enrichment and accumulation of CBM are the result of the coupling effects of sedimentary environment, tectonic evolution, hydrodynamics, geochemistry and other geological factors (Kaiser et al., 1994; Tao et al., 2014b; Yao et al., 2014; Fu et al., 2019; Zhou et al., 2020). Hydrogeological characteristics are also the key factors affecting the generation, migration, enrichment and production of CBM (Scott, 2002; Li et al., 2016; Chen et al., 2021). The groundwater system has dual properties in the enrichment of CBM, which not only promotes the hydraulic migration and dissipation of CBM, but also can form the trap to preserve the CBM (Ye et al., 2001). Qin et al. (2005) proposed that the inactive hydrodynamic condition or stagnant water is benefit for CBM enrichment. The geochemical indicators of produced water can reflect the dynamic state of groundwater, which is an effective parameter for CBM exploration and development (Van Voast, 2003). High TDS groundwater is beneficial to the preservation of CBM in the middle and high-rank coal seams, while low TDS groundwater is favorable for methane production in low-rank coal seams (Liu et al., 2010).

The geochemical characteristics of CBM are also effective indicators for studying genetic types, migration characteristics and gas composition of CBM (Zhang and Tao, 2000). Whiticar (1999) drew the genetic map of CBM based on the relationship between the $\delta^{13}C_1$ and δD values, which has been widely used in the analysis of CBM genesis. In the process of CBM accumulation and reservoir evolution, the fractionation of methane isotope in CBM is widespread, and the methane carbon isotope in the CBM reservoir is often lighter (Qi, 1985; Dai et al., 1986; Bao et al., 2021). In response to this phenomenon, the desorption-diffusion fractionation (Li et al., 2022), the dissolution of flowing groundwater (Qin et al., 2005), secondary biogenic gas mixing (Whiticar, 1999; Tao et al., 2014a), and CO_2 and CH_4 isotope exchange mechanisms, etc. were proposed. The carbon isotope of methane also changes during the tectonic evolution process. Making uplifting for example, with the decrease of reservoir pressure, CBM begins to desorb, and the value of the carbon isotope of methane increases during this desorption process. The increase rate of carbon isotope in different desorption stages is also different.

The purpose of this paper is to discuss the influence of structural, hydrogeological, CBM genesis and carbon isotope characteristics on the CBM accumulation and production, to play a guiding role in the exploration and development of CBM and CO_2 geological storage in the Daning-Jixian block.

2 Geologic setting

2.1 Structural background

The Daning-Jixian block is a monoclinic structure inclined to the west as a whole, but the local structural characteristics are significantly different (Fig. 1). A fault structure zone was developed in the center part, mainly consisting of the Xueguan-Yukou thrust fault and its associated secondary fault, which runs across the study area in NE-SW direction. In addition, a regional anticline (Guyi-Yaoqu anticline) was also developed in this center part, which was formed by the traction of faults. The tectonic amplitude is range from 80 to 120 m in this anticline zone, and the axis length is about 40 km. Otherwise, there are some small tensional normal faults developed in the eastern part of the Daning-Jixian block. Based on the tectonics shape feature, our study area can be divided into four structural domains: a broad and gentle slope zone (B1) in the south-east, a depressional area (B2) in the north-east, an anticline and fault zone (B3) in the center part and a slope zone (B4) located in the west (Fig. 1).

2.2 Coal stratigraphy

The main coal-bearing strata in the Daning-Jixian block are the Taiyuan Formation of Carboniferous and Shanxi Formation of Permian (Fig. 2). There are multi-coal seams (No. 1 to No. 8) developed in this area. No. 5 coal seam and No. 8 coal seam are the main coal seams for CBM commercial development which are stably distributed in this area. The thickness of No. 5 coal seam in the Shanxi Formation ranges from 0.5 to 8 m, with an average thickness of 3.3 m and a burial depth from 793 m to 1289 m. The thickness of No. 8 coal seam in the Taiyuan Formation ranges from 3 to 9.8 m, with an average thickness of 4.1 m and a burial depth from 881 m to 1375 m. The tectonic evolution of coal strata was influenced by three phases of tectonic movements: the Indosinian movement, Yanshannian movement and Himalayan movements (Zhang et al., 2001; Tian, 2012; Wang et al., 2013; Wang, 2014).

2.3 Hydrogeology

Four sets of aquifers exist from bottom to top in the study

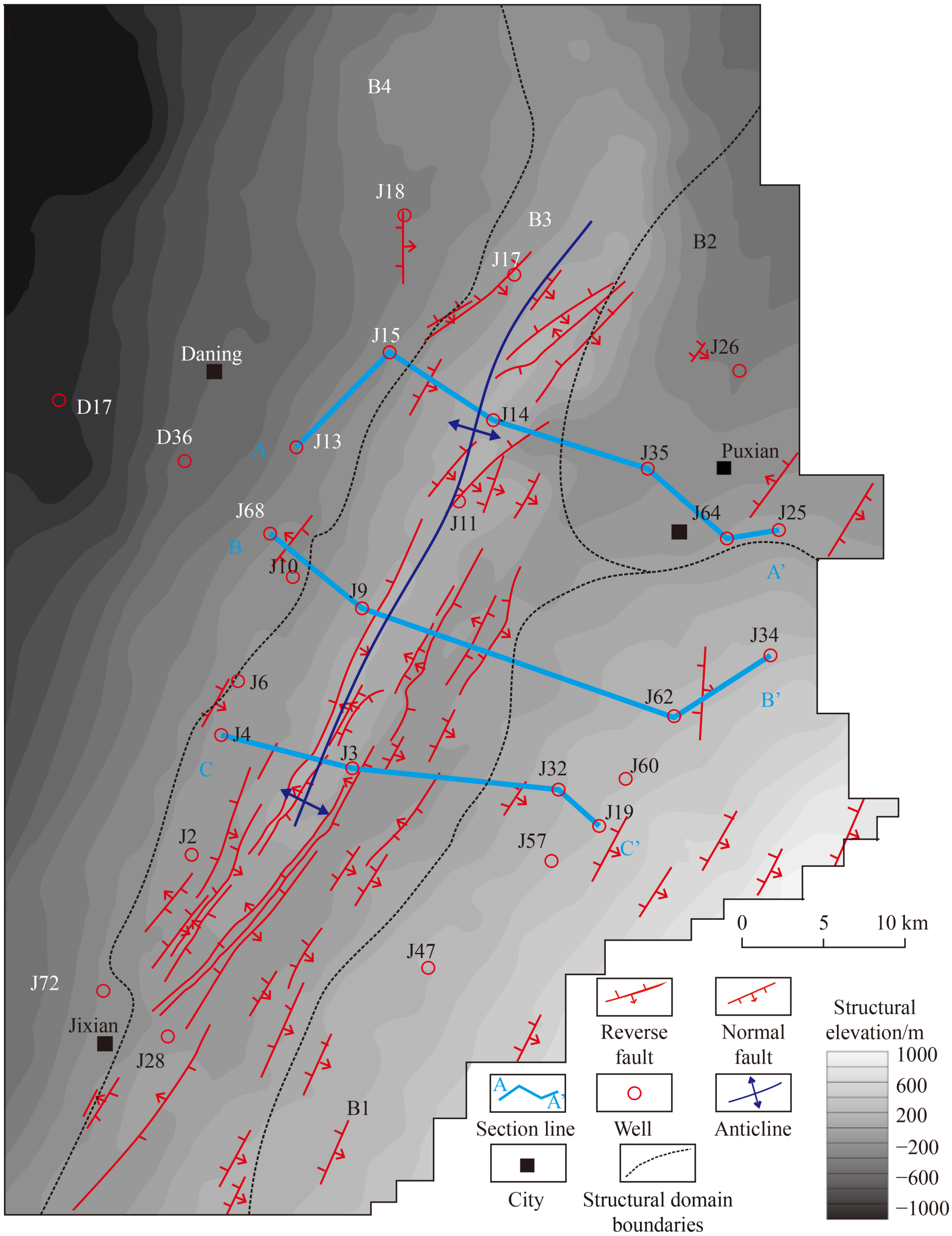

Fig. 1 The geological structure image of No. 8 coal seam in the Daning-Jixian block.

area: Cambrian-Ordovician, Carboniferous, Permian and Quaternary (Fig. 2). The Carboniferous and Permian clastic rock aquifers and Quaternary loose aquifers are weak aquifers, and the Cambrian-Ordovician aquifers are water-rich strata, which is carbonate fractured karst aquifers (Wang, 2016; Chen et al., 2021). The Quaternary aquifer is far from the coal seam, mainly controlled by the terrain, with less influence on the production of water and gas in coal strata (Yao et al., 2014). The sandstone aquifer of the Shanxi Formation and limestone aquifer of the Taiyuan Formation have direct influence on the production of water and gas. The direct roof and floor of the No. 5 coal seam in the Shanxi Formation is mudstone, containing sandy mudstone, which has played a role in blocking the aquifer in Shanxi Formation. The roof and floor of No. 8 coal seam in the Taiyuan Formation are limestone aquifers, with abundant water content and high permeability, which are demonstrated have a strong transformation effects on CBM.

3 Materials and methods

3.1 Sample and experiments

Produced water samples from 15 CBM production wells were collected for the determination of the TDS and ion composition in the produced water. These water samples

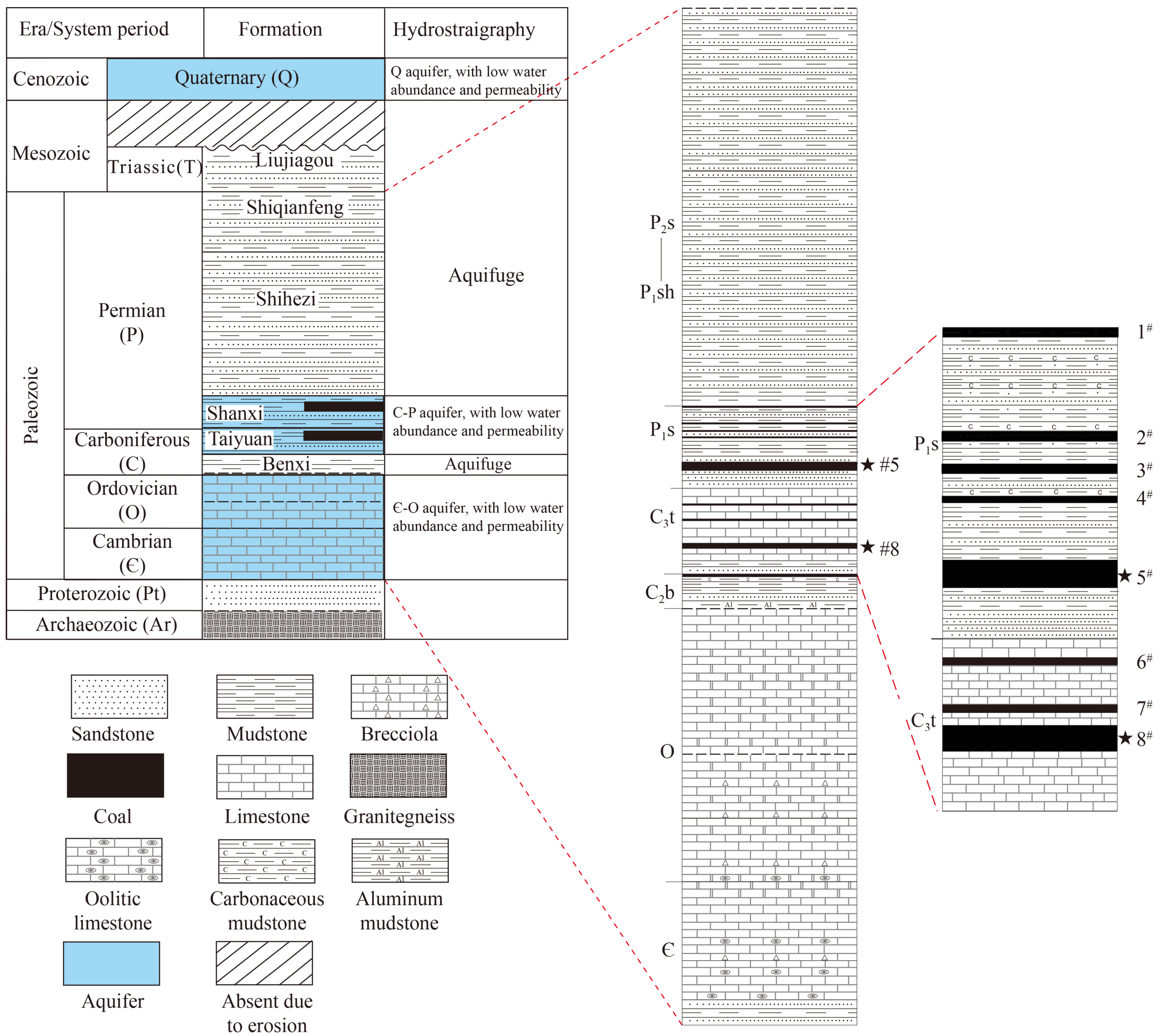

Fig. 2 Delineation of the characteristics of stratigraphy and hydrostratigraphy in the Daning-Jixian block.

were all collected from the CBM production wells which have experienced more than 350 days of drainage. To avoid the influence of inter-well interference, the distance between adjacent sampling wells was greater than 550 m to ensure that the produced water could truly reflect the hydro-chemical characteristics of formation water (Zhang et al., 2015; Yan et al., 2015). The water samples were collected in polyethylene bottles which have been rinsed three times using the produced water. The chemical composition and TDS of the produced water from the CBM wells were determined following MT/T 202-2011 and GB/T 6920-1986 standards respectively.

The gas samples were collected from No. 5 coal and No. 8 coal CBM wells respectively for the carbon isotope and composition tests. Gas composition and stable carbon isotope measurements were carried out following GB/T 10628-2008 and GB/T 6041-2002 standards at Lanzhou Institute of Geochemistry, Chinese Academy of Sciences.

3.2 Method

The flow direction of groundwater can be represented by hydraulic-head, which can be obtained directly from the injection-pressure drop test well. In fact, many CBM production wells have not carried out pressure recovery well testing. Therefore, the water head is estimated according to the Bernoulli equation in our research. Taking the sea level as the datum plane, the formula of water head height is as follows:

$$H = Z + \frac{P}{\rho g} + \frac{av^2}{\rho g}, \tag{1}$$

where H is the total hydraulic head (m), Z is the position hydraulic-head (m), $\frac{P}{\rho g}$ represents the pressure hydraulic head (m), and $\frac{av^2}{\rho g}$ represents the average flow velocity hydraulic head (m).

4 Results and discussion

4.1 Geochemical characteristics of produced groundwater

Table 1 presented the statistical results of the hydrochemical parameters of groundwater in the study area. Na^+ is the most prevalent cation in the Daning-Jixian block, which is much higher than other cations, followed by Ca^{2+} , Mg^{2+}, and K^+. The anion were $Cl^- > HCO_3^- > SO_4^{2-}$ in the study area. In general, the ions of the produced water in the study area are dominated by Na^+, Cl^-, and HCO_3^-, with a lack of SO_4^{2-}. As shown in Fig. 3, the water type in the study area was dominated by Cl^-Na and $HCO_3 \cdot Cl^-Na$. The water type near Well J19 is mainly $HCO_3 \cdot Cl^-Na$, and the water type near Well J2 is mainly Cl^-Na.

Usually, SO_4^{2-} is enriched in an open environment which is strongly affected by atmospheric precipitation

Table 1 Ion concentration of water from CBM Well

Sampling	K^+/(mg·L^{-1})	Na^+/(mg·L^{-1})	Mg^{2+}/(mg·L^{-1})	Ca^{2+} /(mg·L^{-1})	HCO_3^- /(mg·L^{-1})	SO_4^{2-}/(mg·L^{-1})	CO_3^{2-}/(mg·L^{-1})	Cl^-/(mg·L^{-1})
J1-03	13.3	2134	43.7	106.0	852	177.0	0.0	3451
J1-10	14.3	2720	42.1	83.5	1404	12.9	91.9	3464
J2-14	11.9	2212	34.5	76.4	1600	4.6	0.0	2828
J2-22	33.3	2722	32.9	84.3	704	<0.09	30.7	4055
J2-34	94.6	2589	31.8	153.0	1420	<0.09	0.0	3618
J2-36	32.9	3346	52.6	210.0	1224	<0.09	34	5079
J2-56	68.1	4062	61.5	263.0	1043	<0.09	0.0	6074
J4	14.8	2944	44.2	90.3	1701	<0.09	60	3906
J10	15.2	3370	39.4	133.0	308	6.0	0.0	5150
J19	10.1	1057	13.5	22.4	1838	<0.09	67.9	589
J19-4	17.3	1535	30.1	54.6	11.7	<0.09	0.0	2447
J19-7	43.9	3648	56.0	220.0	271	<0.09	0.0	6312
J19-8	11.0	768	9.0	35.0	1490	<0.09	47.9	294
J68	45.6	5998	130.0	189.0	967	<0.09	0.0	9805
JS5-2	15.3	2673	41.6	95.1	1411	<0.09	76.5	3412

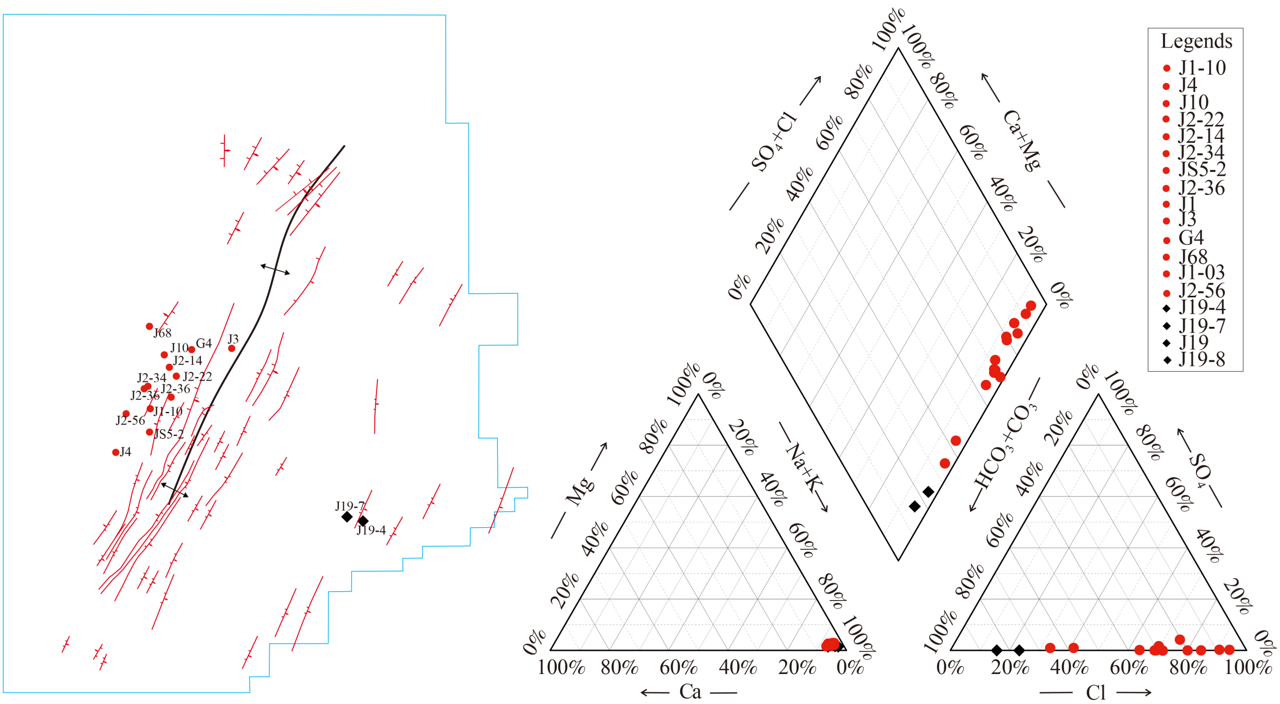

Fig. 3 Trilinear diagram showing the relative distribution of major ions (in meq/L) of produced water in the Daning-Jixian block.

and surface water recharge. Groundwater rich in Na^+, K^+, and HCO_3^- represents a semi-open environment. Mg^{2+} and Ca^{2+} are closely related to the closed groundwater environment (Li et al., 2014; Chen et al., 2021). Therefore, the groundwater of coal seam is weakly connected to surface water in this area. The groundwater in the eastern part of the study area is in semi-open environment, while the groundwater activity in the western part is a closed-semi-closed environment.

The genetic type of groundwater can be identified by groundwater hydrogen and oxygen isotope (Michael et al., 2008), and the genesis of water is related to the groundwater isotope characteristic (i.e., hydrogen and oxygen isotope) and local meteoric water line (LMWL). The local meteoric water line equation of the Ordos Basin is (Hou and Zhang, 2008): D = 6.88 ^{18}O + 0.23 (r = 0.9485). The isotopic composition of most groundwater sample plots basically falls near the atmospheric precipitation curve (Fig. 4), indicating that the produced water in the study area are mainly from atmospheric precipitation, especially in the area around Well J19.

It is noted that the data point from the area around Well J2 deviates to the right from the LMWL. The ^{18}O deviation may be related to seawater mixing, evaporation and fluid-rock interaction under high temperatures (Sheppard, 1986; Taylor, 1997; Kinnon et al., 2010). Considering the groundwater recharge environment in this area, the ^{18}O deviation phenomenon may be caused by the interaction between fluid and rock during groundwater runoff.

4.2 Hydrodynamic characteristics

Total dissolved solids (TDS) are often used to reflect the activity of groundwater. Usually, high TDS represents a closed environment with inactive groundwater, and low TDS represents an open environment with relatively active groundwater (Wang et al., 2007; Chen et al., 2019). The TDS of produced water in the study area was diversified, varying in range of 1000 mg/L to 16946 mg/L (Fig. 5), and increases from east to west. The TDS indicates two types environment of groundwater in this area. In the east part of the study area, the groundwater is dominated by $HCO_3 \cdot Cl^-Na$-type water, with relatively low TDS which increases slowly from east to west, indicating a semi-open groundwater environment with relatively active groundwater alternation. For the west part (i.e., the west of the fault zone), the TDS increased sharply, and the water type is dominated by Cl^-Na-type water, indicating a relatively closed environment with stagnating groundwater flow. Generally, this area can be divided into two hydraulic units (i.e., the recharge-runoff zone in the east and the weak runoff-stagnation zone in the west).

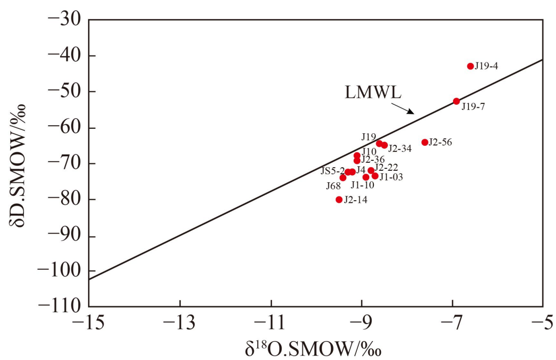

Fig. 4 Plot of δ^{18}O vs. δD for produced water from the Daning-Jixian block and its relation to the local meteoric water line (LMWL).

The hydraulic head, calculated by Eq. (1), ranges from 400 m to 1250 m in the study area (Fig. 6). The Heilongguan fault area in the east of the study area is the main recharge area of the Daning-Jixian block. Thus, the eastern margin of the study area is characterized by the highest hydraulic head and strong groundwater energy. Affected by the terrain, Groundwater generally flows from east to west in the Daning-Jixian block and enters the pressure retention area in the west of the fault zone (Fig. 6). The intensity of groundwater runoff gradually decreases from east to west. Two higher hydraulic head values exist in this area, which are the area near Wells J32 and J19 in the east of the fault zone and the area near Wells J68 and J10 in the west of the fault zone, respectively. The higher hydraulic-head in the area near Wells J32 and J19 is caused by the influence of the Heilongguan fault recharge area, while the higher hydraulic head in the area near Wells J68 and J10 may be affected by the connection of other strong aquifers and coal seam which caused by a local fault. A statistical method proposed by Yan (2016) was used to analyze the frequency distribution of the TDS. The TDS in the study area showed a single normal distribution with an overall slope of the cumulative distribution curve of 0.79 (Fig. 7), indicating a uniform groundwater system in the study area.

4.3 Thermal maturity of the coals

The rank of No. 5 coal seam ranges from medium-volatile bituminous to semianthracite with R_o range from 1.3% to 2.7%, while the rank of No. 8 coal seam ranges from low-volatile bituminous to semi-anthracite with R_o range from 1.5% to 3.2%, R_o. Vertically, No. 8 coal shows a higher degree of metamorphism than No. 5 coal. The maturity distribution characteristic of these two sets of coal seams is basically the same, gradually increasing from east to west-south-west, showing strong anisotropy (Fig. 8).

4.4 Geochemical characteristics of produced gas

4.4.1 Characteristics of the gas composition

The molecular composition of the produced gas in the study area is dominated by CH_4 (Fig. 9), with a methane concentration greater than 94% in No. 5 coal seam and

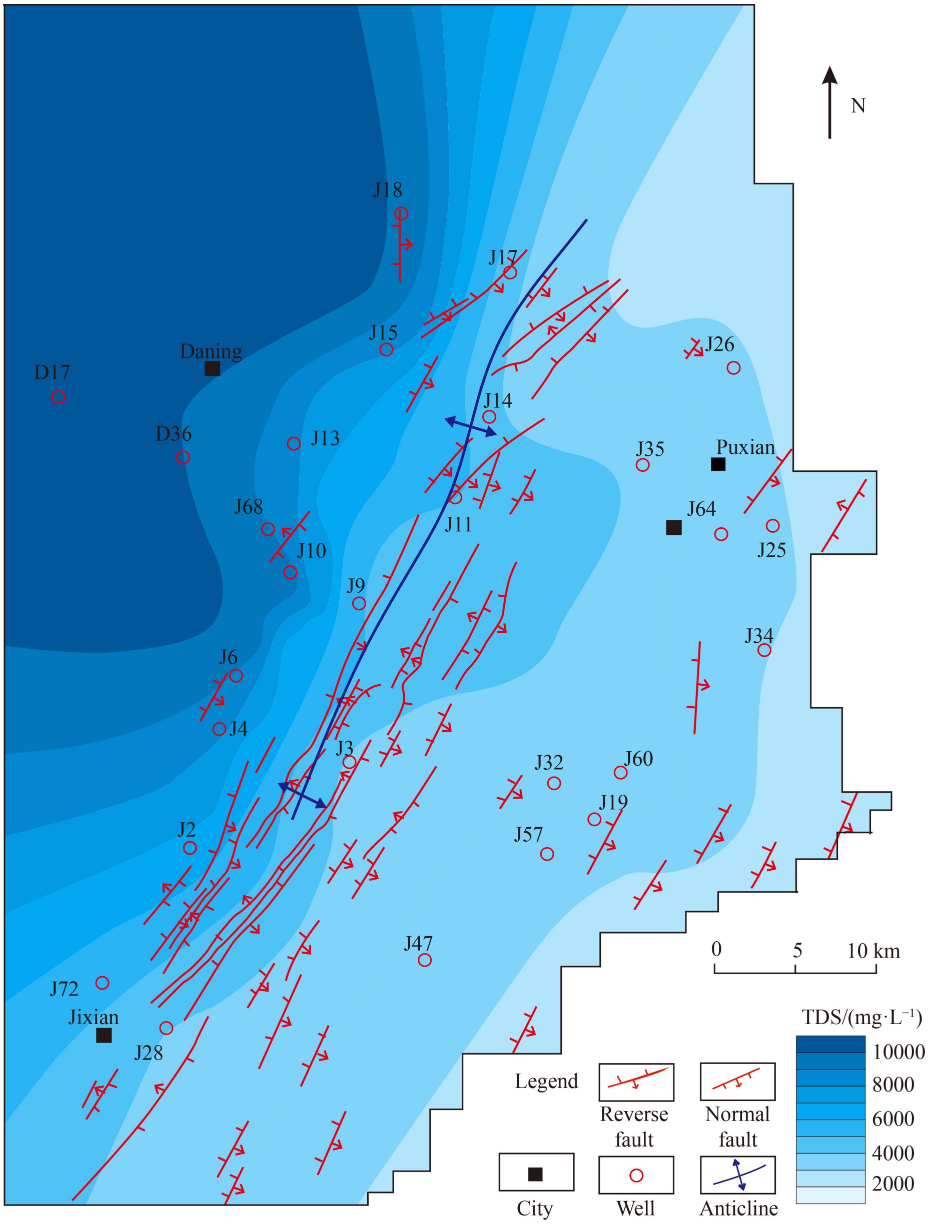

Fig. 5 Isolines of the total dissolved solids in the Daning-Jixian block.

greater than 81% in No. 8 coal seam. There also contain small amounts of C_{2+}, N_2, and CO_2 in these produced gases. The percentage of C_{2+} is particularly low (0−0.45% in No. 5 coal and 0−1.3% in No. 8 coal).

The concentration of N_2 in No. 5 coal seam ranges from 0.45% to 4.49%, with an average of 1.97%, while the concentration of CO_2 ranges from 0.01% to 1.18%, with an average of 0.65%. The concentration of N_2 in No. 8 coal seam ranges from 0.55% to 14.29%, with an average of 3.08%, while the concentration of CO_2 ranges from 0.74% to 3.59%, with an average of 1.64%. The drying coefficients ($C_1/C_{1–5}$) of these two sets of coal seams are in the range of 0.98−1 and greater than 0.95, indicating that the produced gas is characterized by dry gas (Liu et al., 2014).

4.4.2 Characteristics of isotopic composition

The $\delta^{13}C_1$ value of No. 5 coal seam ranges from −56.07‰ to −31.5‰, with an average value of −41.55‰. The $\delta^{13}C_1$ value of No. 8 coal seam ranges from −56.03‰ to −27.43‰, with an average value of −41.67‰. The $\delta^{13}C_1$ values in the eastern part of the study area are generally less than those in the central or western parts (Figs. 1 and 10). The highest $\delta^{13}C_1$ values distributes in the area near Well J13 which is located in the slope zone of the B4 block, while the lowest values appear in the area near Wells J17 and J25 (Figs. 1 and 10). Vertically, the difference in $\delta^{13}C_1$ values between No. 5 and No. 8 coal seams is not obvious in the study area, but the D-value between these two coal seams varies in different tectonic units. Within the eastern depression

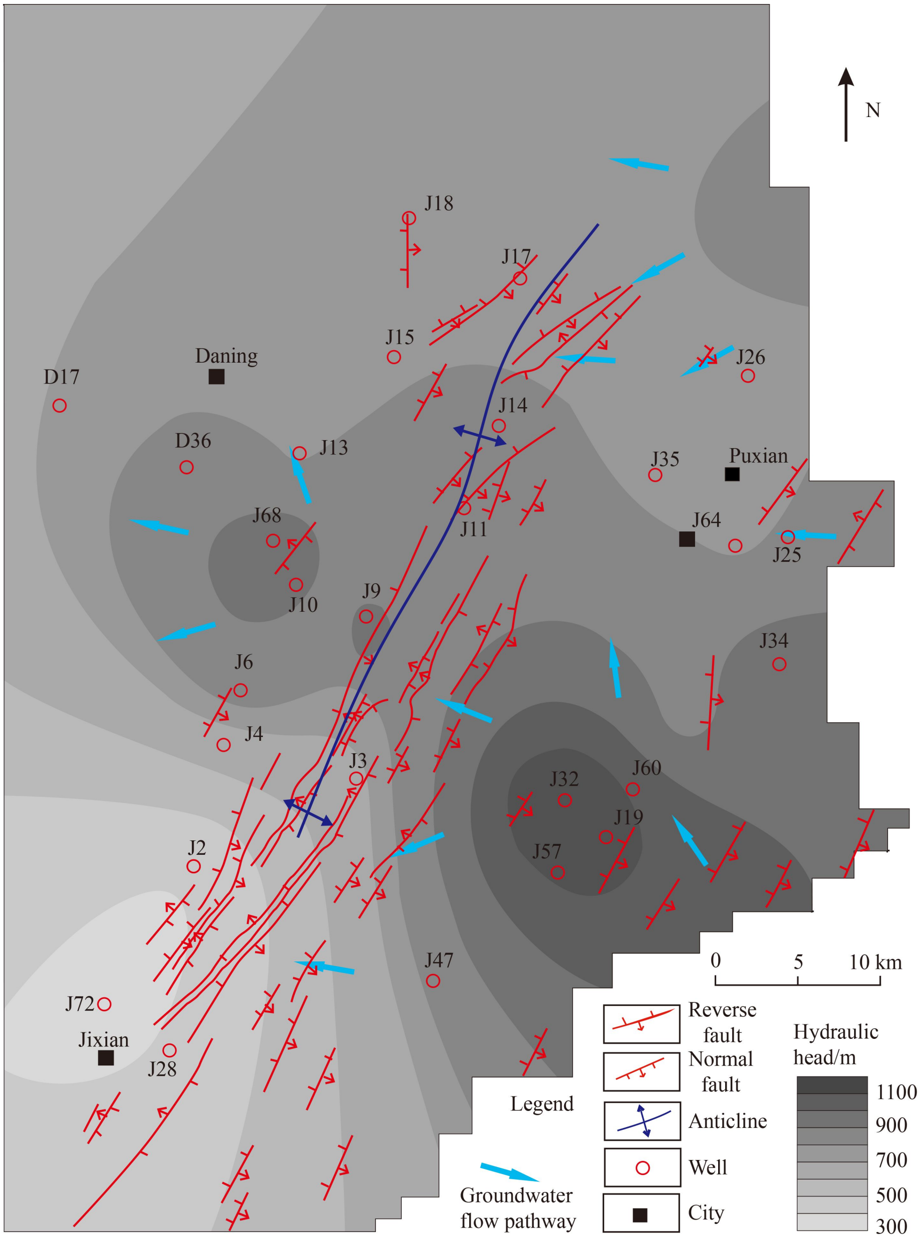

Fig. 6 Isolines of the hydraulic head in the Daning-Jixian block.

and slope zone, the $\delta^{13}C_1$ values for No. 5 coal seam are generally lighter than those for No. 8 coal seam, with an exception of Well J65, while in the central anticline uplift zone and western slope zone showing an opposite phenomenon.

As $^{13}CH_4$ is more polar than $^{12}CH_4$, $^{13}CH_4$ is more easily dissolved and taken away than $^{12}CH_4$. The depression and slope zone in the east is located in the recharge and runoff area with strong groundwater dynamics. No. 8 coal seam has stronger hydrodynamics than No. 5 coal seam due to being connected to limestone fissure water in the study area. Otherwise, the hydrodynamics of the lower coal group in north China tend to be stronger than that of the upper coal group (Qin et al., 2006). As a result of these comprehensive effects, a lighter carbon isotope in No. 8 coal seam than in No. 5 coal seam was manifested in the eastern depression and slope zone. For the western part of study area, which is in a weak runoff and stagnation zone, groundwater has less influence on the fractionation of methane. The distribution characteristic of the $\delta^{13}C_1$ value is basically consistent with buried depth, showing a positive correlation trend (Li et al., 2014).

Thermal simulation experiments have shown that the maximum vitrinite reflectance has a good positive correlation with $\delta^{13}C_1$ (Dai et al., 1986; Liu et al., 2003; Duan et al., 2014). CH_4 originates from the destruction of C-C molecular bonds during the thermal evolution of coal. ^{12}C-^{12}C with the lowest bond energy is easier broken compared with ^{13}C-^{13}C which has higher bond

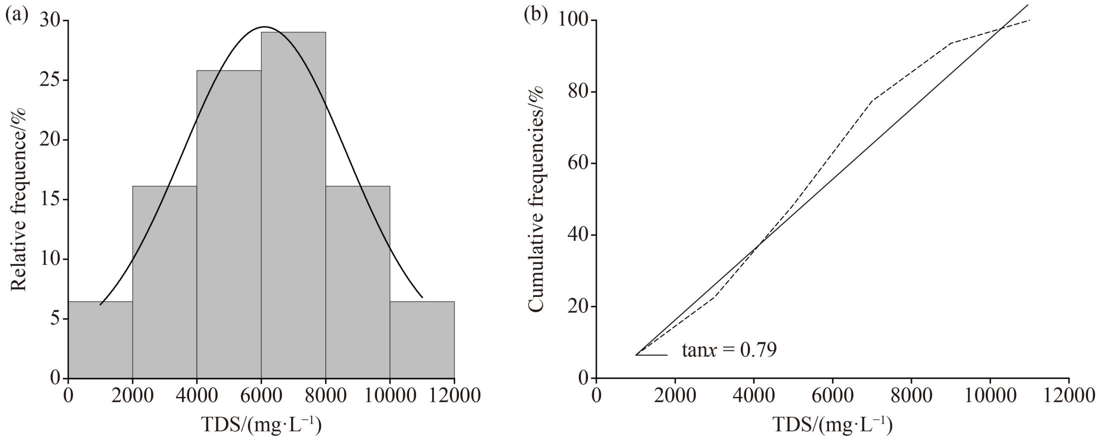

Fig. 7 Statistical characteristics of TDS in the Daning-Jixian block. (a) TDS frequency histogram. (b) TDS cumulative frequency distribution.

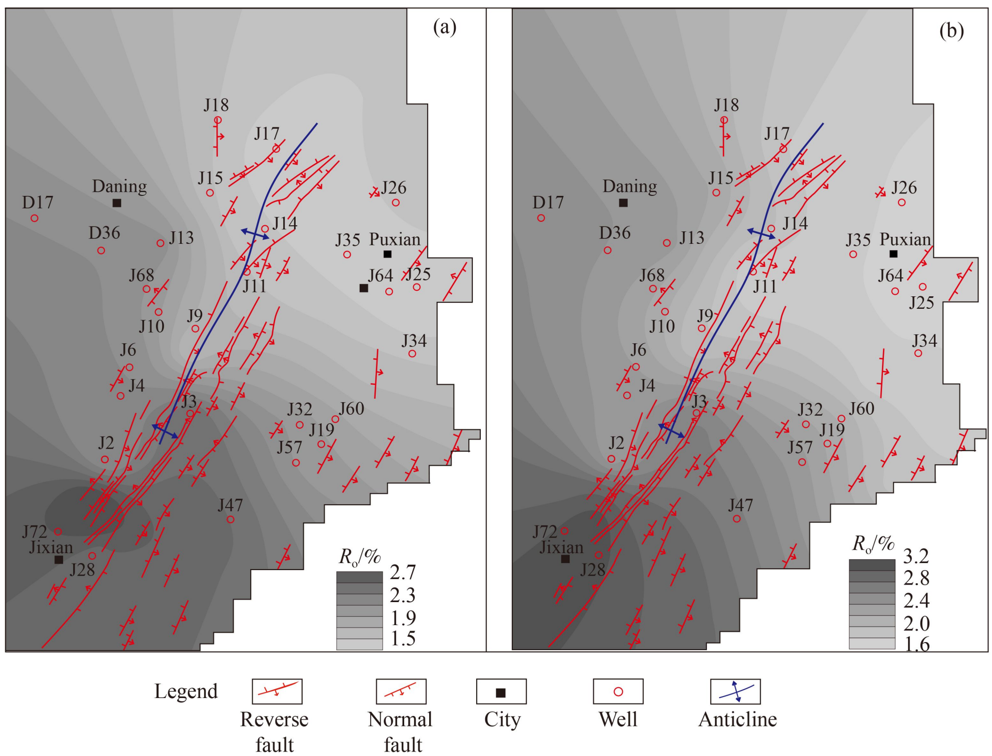

Fig. 8 Map of vitrinite reflectance in the Daning-Jixian block. (a) No. 5 coal seam, (b) No. 8 coal seam.

energy. Therefore, $^{12}CH_4$ is preferentially produced in the initial stage of thermal evolution. Then, with the increase of thermal evolution degree, $^{13}CH_4$ is gradually produced which results in a heavier gas $\delta^{13}C_1$ value. As shown in Fig. 11, the R_o has a positive correlation with $\delta^{13}C_1$ in the study area. Compared with the previous thermal simulation experiments, the $\delta^{13}C_1$ value of the two sets of coal seams is significantly less, and the difference between the actual $\delta^{13}C_1$ value and the ideal simulation experiment value decreases as the R_o increases (Fig. 11). The maturity of the coal rocks in study area gradually increases from east to west-south-west (Fig. 8). Therefore, the large D-value between the actual $\delta^{13}C_1$ value and the ideal simulation experiment value may be caused by the isotopic fractionation in the eastern part of the study area, as a result of strong hydrodynamic conditions.

4.4.3 Origin of the coalbed methane

The $\delta^{13}C_1$ demarcation value of biogenic gas and thermogenic gas is −55‰. The $\delta^{13}C_1$ value of biogenic gas is generally less than −55‰, while thermogenic gas is generally greater than −55‰ (Whiticar, 1999). With the increase of thermal evolution degree, the $\delta^{13}C_1$ value will gradually become heavier (Duan et al., 2014). As shown in Fig. 12, two wells (i.e., Wells J17 and J25) exist in the

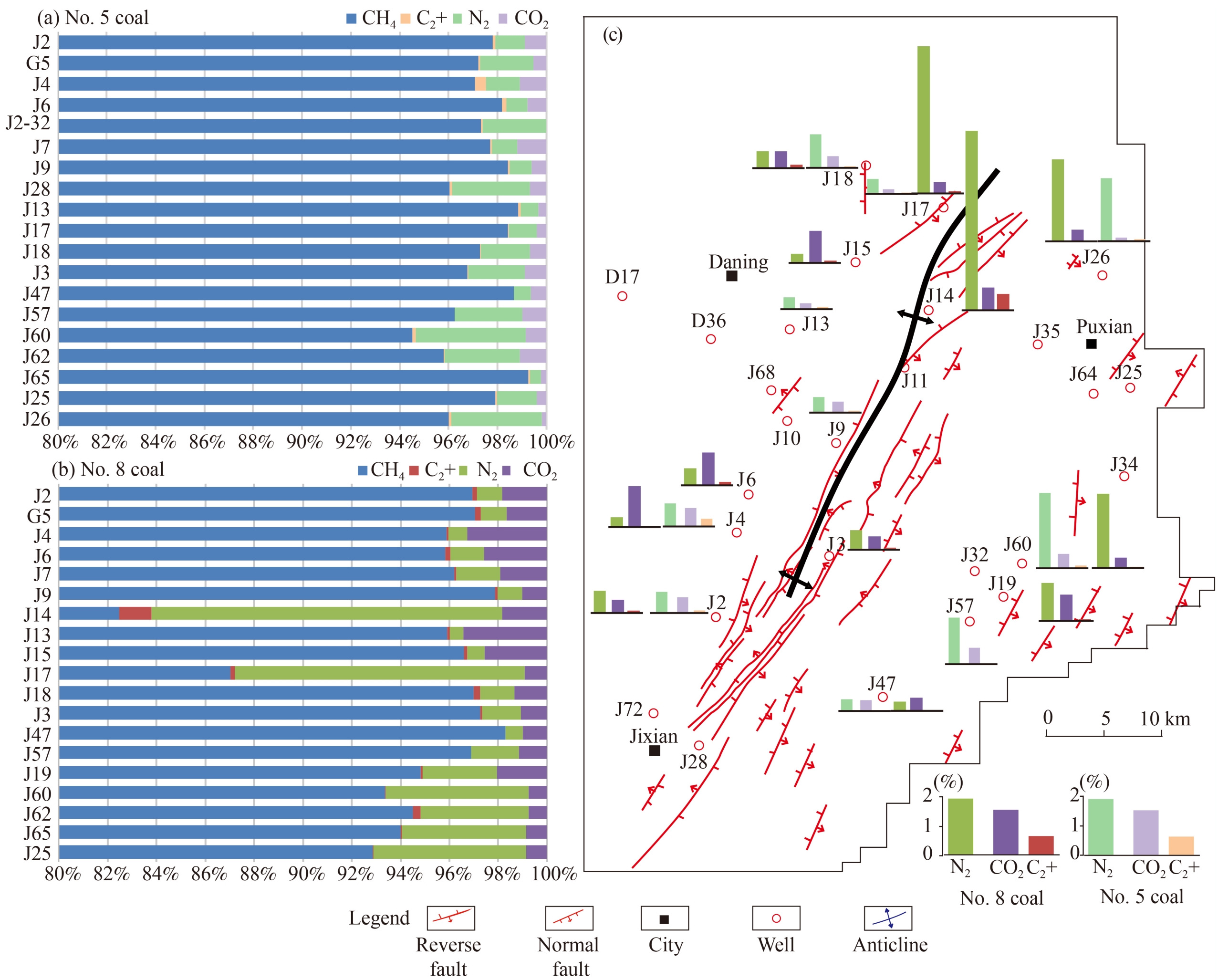

Fig. 9 Diagram of the molecular composition of gas samples from CBM wells in the Daning-Jixian block. (a) The molecular composition of gas samples from No. 5 coal seam. (b) The molecular composition of gas samples from No. 8 coal seam. (c) The distribution of the concentration of N_2, CO_2, and C_2^+.

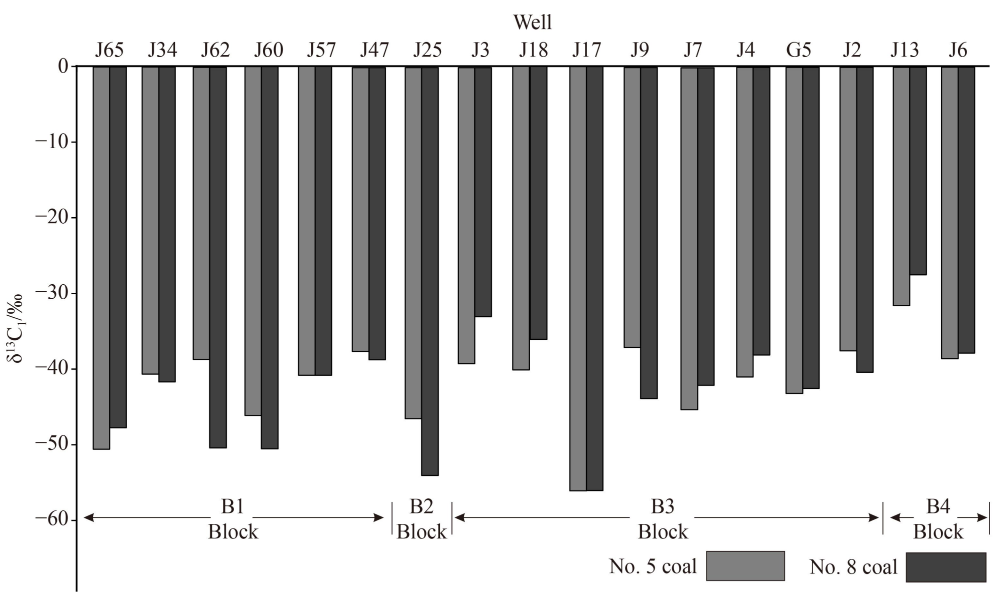

Fig. 10 The $\delta^{13}C_1$ values of the produced gas from CBM wells in the Daning-Jixian block.

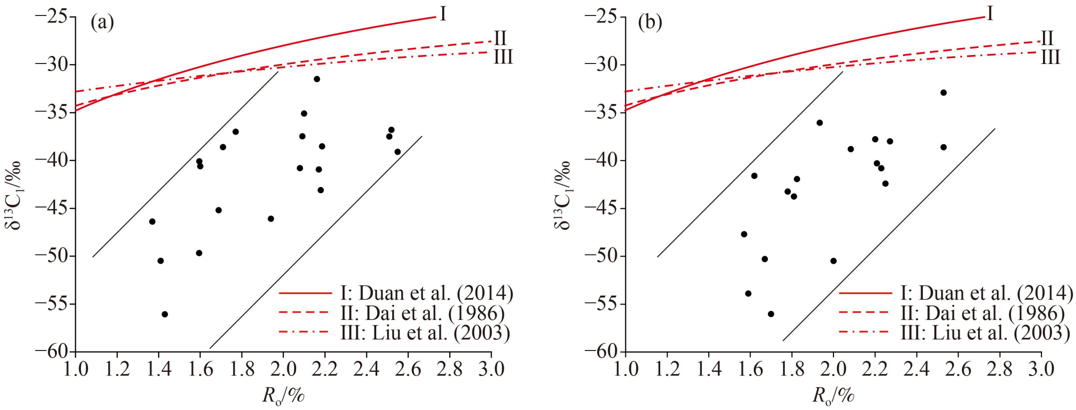

Fig. 11 The relationship between R_o and $\delta^{13}C_1$. (a) No. 5 coal seam; (b) No. 8 coal seam.

biogenic gas zone which indicates a secondary biogenic gas origin in the eastern edge of the study area. As these wells (Wells J17 and J25) have low TDS and locate close to water recharge areas, methanogens carried into the coal seam by groundwater could be an explanation for this biogenic gas generation (Ye et al., 2001). The data points of the remaining wells fall within the zone of transport-diffusion-fractionation, which indicates a migration of thermal-related gas. Therefore, the CBM is predominantly thermogenic which has generally undergone transport-diffusion after generation, followed by secondary biogenic gas which is mainly distributed in the eastern edge of the study area (e.g., the area near Wells J17 and J25).

4.5 Gas content and migration of coalbed methane

The gas content of No. 5 and No. 8 coal seams in the Daning-Jixian block is in range of 7.24−17.95 m^3/t and 3−20 m^3/t, respectively. As shown in Fig. 13, gas content generally increases from east to west in the study area, which is basically consistent with the distribution of the coal organic matter maturity. The gas content in the area near Well J17 is very low, which may be caused by the development of faults and the active hydrodynamic there. As shown in Fig. 14, the gas content has a positive correlation with TDS and a negative correlation with hydraulic-head, indicating that the transport and enrichment of CBM were affected by groundwater and the distribution of gas content in the study area is closely related to hydrodynamics.

As discussed in Section 4.4, the fractionation of carbon isotopes is mainly influenced by hydrodynamics. The carbon isotope distribution can effectively indicate the gas migration path. The gas content distribution is basically consistent with the isotope distribution in the study area. In the east of the fault zone, the CBM is carried by groundwater to the runoff zone in the west. In

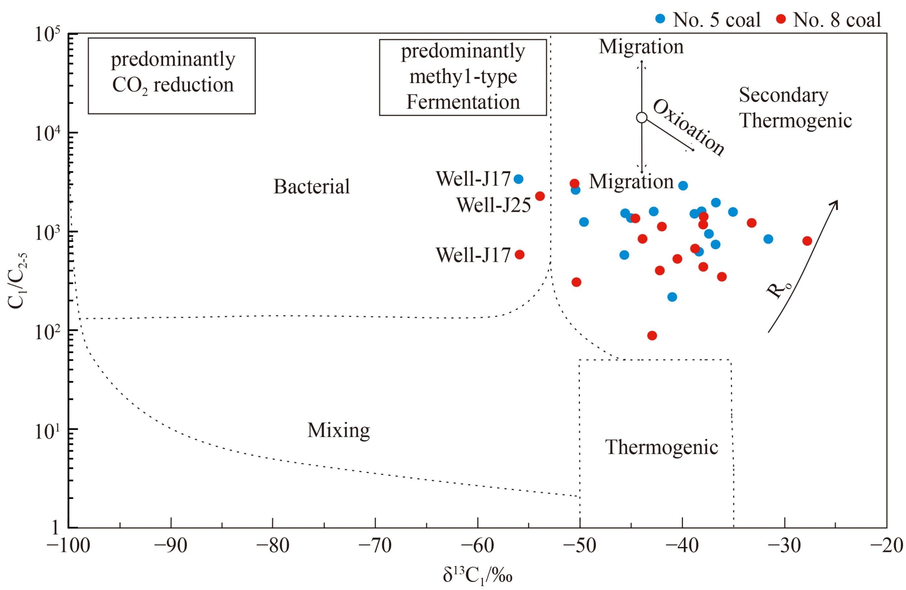

Fig. 12 Map of genetic types of coalbed methane.

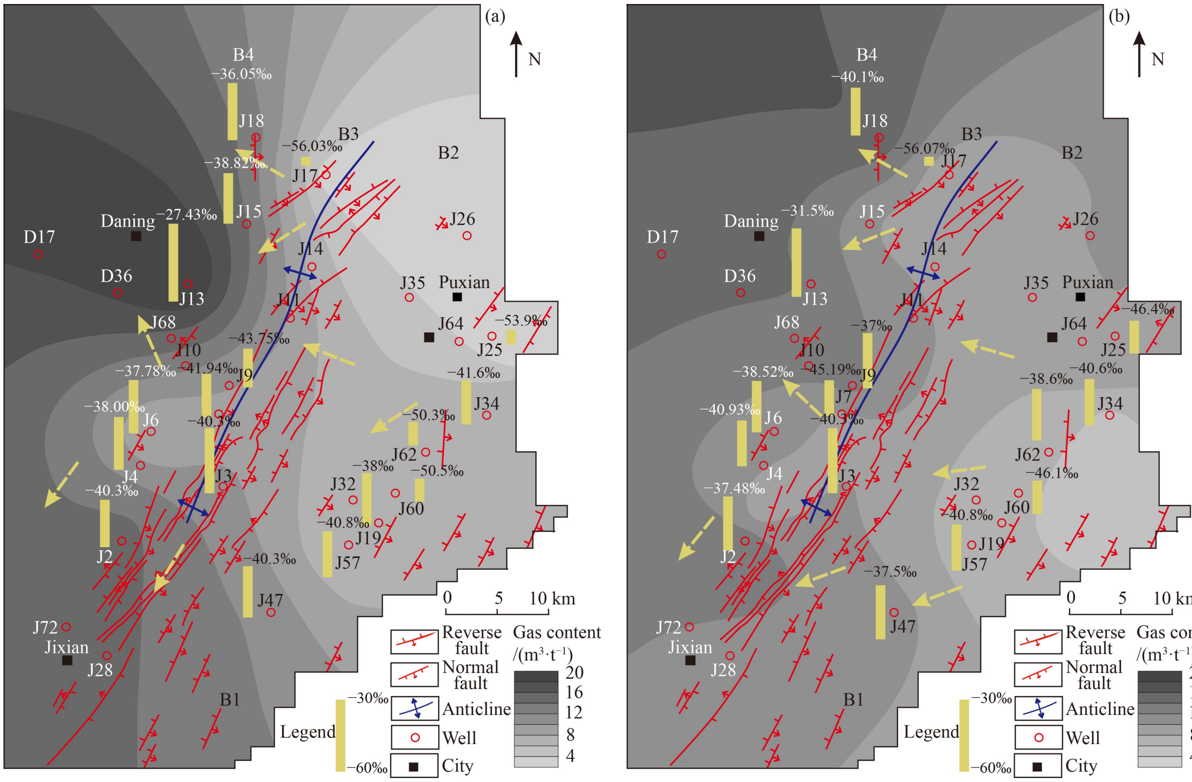

Fig. 13 The distribution of gas content and carbon isotopes in the Daning-Jixian Block. The yellow arrows indicate the migration of gas. (a) No.5 coal seam. (b) No.8 coal seam.

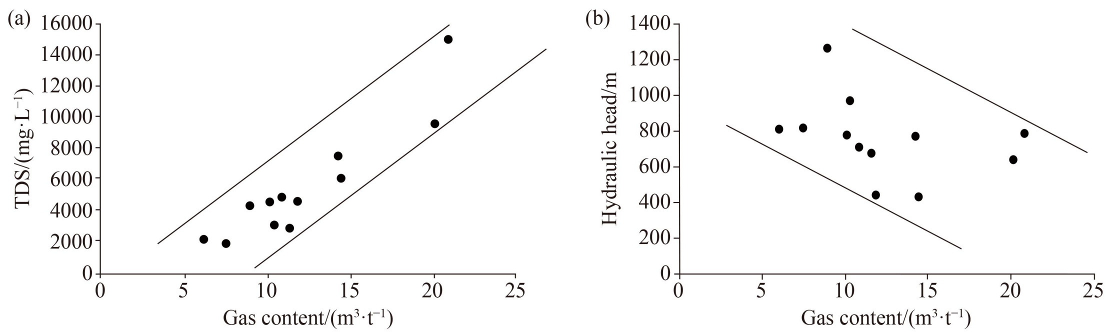

Fig. 14 (a) The relationship between gas content and TDS. (b) The relationship between gas content and hydraulic head.

the reverse fault zone, which is formed under a compression environment, the coal reservoir always has relatively higher pressure and good sealing condition (Chen et al., 2019). The methane carried by groundwater could be reabsorbed and preserved in coal seam near these fault zone (Qin et al., 2006). So, in the area that is located east to the fault zone, the gas content increases gradually from east to west. In the west of the fault zone, the high TDS value indicates that the groundwater is in a closed environment (e.g., mainly in the stagnant and weak runoff zones). The organic matter maturity has shown a dominant influence on gas carbon isotope, which gradually becomes heavier westward. In this area, the role of groundwater is mainly acted as a seal on CBM. In general, CBM content is mainly controlled by both effects of hydrodynamic and tectonic in the study area.

4.6 Gas accumulation and implication for coalbed methane production

The distribution of CBM is mainly controlled by geological and hydrological factors (Scott, 2002; Yao et al., 2013). According to the previous section, the coal seam gas had undergone migration-diffusion effects, which are affected by thermal evolution, groundwater dynamic conditions and structural characteristics. Through the comparison of three profiles (i.e., A-A', B-B', and C-C') from north to south in the study area (Figs. 1, 15, 16, and 17), two modes were proposed to explain the accumulation and enrichment of CBM in this area. One in which CBM is carried to the deeply buried area while groundwater transportation and reabsorbed when it encounters impermeable boundaries, which forms a compound CBM reservoir with hydrodynamic and fault sealing. And the other in which a large number of thermogenic gases generated by coal organic matter with high thermal evolution is blocked by fault zones and enriched in a stagnant and weak runoff hydrodynamic area.

The enrichment characteristics of CBM in the east of the fault zone area can be explained by the first model. In profile A-A' (Fig. 15), in the eastern edge of the study area (e.g., Well J25), which was subjected to strong hydrodynamic, the CBM preservation condition is relatively poor and gas content is low even though secondary biogenic gas works as a supplement there. The gas migrated along with the groundwater while it ran westwards, which led to a significant increase of gas content in Wells J64 and J35. Due to the barrier of the reverse fault, the reservoir pressure increases, and the migrated gas is reabsorbed and preserved here. The lateral sealing of the reverse fault effectively blocked the diffusion of gas, which led to a relatively higher gas content in the footwall area of the fault. It is noted that the lateral variation of gas content in the No. 8 coal seam in section A-A' is more obvious than in the No. 5 coal seam (Fig. 15), as a result of the influence of limestone aquifer. The enrichment mode of gas content in A-A' is also applicable in the other two profiles.

The mechanism of the CBM enrichment in the west of the fault zone could be explained by the second mode. The higher TDS indicated a stagnant state environment of the groundwater in this deeply buried area. The thermal evolution degree of coal organic matter was higher in here. More $^{13}CH_4$ was generated accompanied by a larger $\delta^{13}C_1$ value (Figs. 15, 16, and 17). The generated methane gas is blocked by the reverse fault, which prevents the gas from escaping upwards (e.g., Wells J15 and J13 in profile A-A', Wells J9 and J68 in profile B-B', and Well J4 in profile C-C'). Eventually the coal seam methane is accumulated in the slope zone.

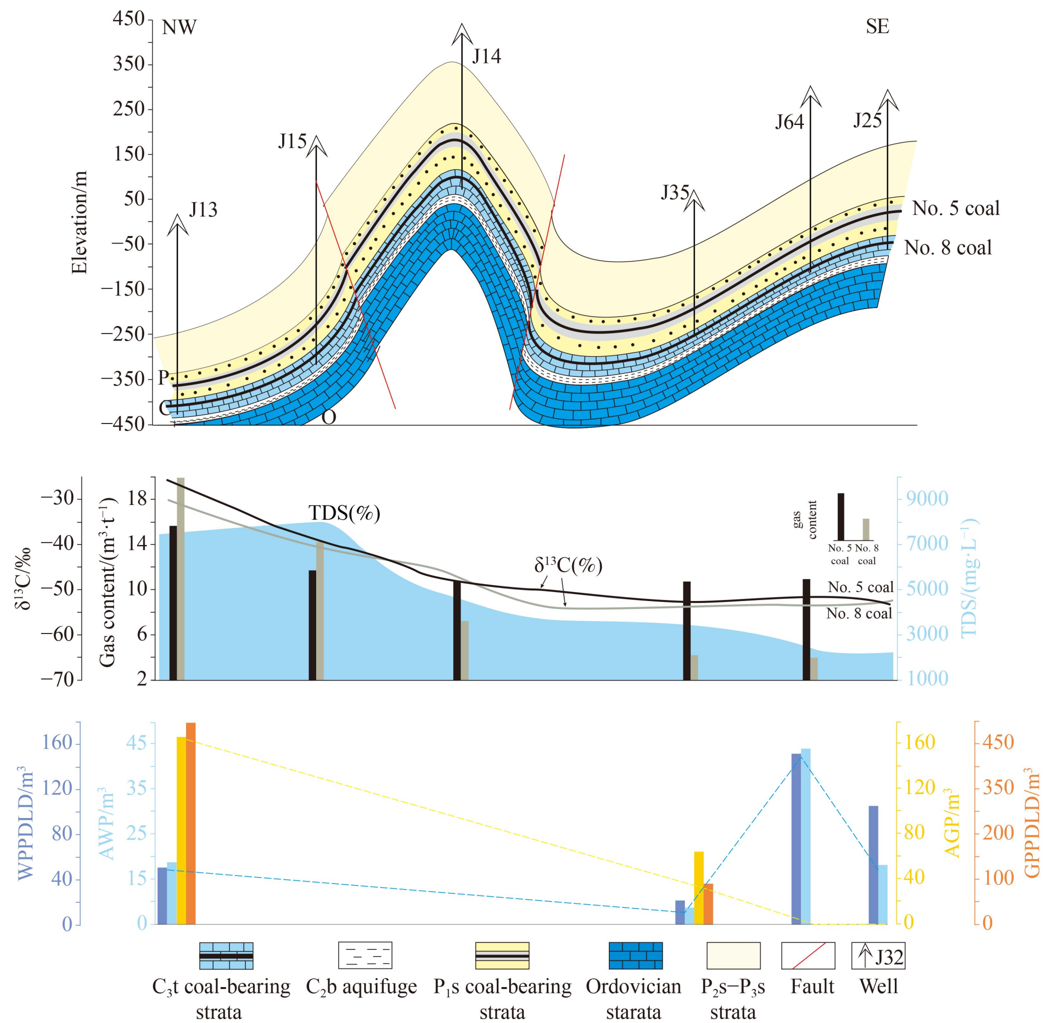

Fig. 15 The characteristic of gas accumulation and production in profile A-A' (TDS is total dissolved solids, AWP is the average of water production, AGP is the average of gas production, WPPDLD is the water production per unit dynamic liquid level drop, GPPDLD is the gas production per unit dynamic liquid level drop).

CBM production performance is influenced by gas content, reservoir pressure, hydrodynamic conditions, etc. (Moore, 2012). The wells controlled by these two different reservoir accumulation models described above have different production characteristics.

In the area that locates in the east of the fault zone, which following the first model, production wells are subject to active groundwater dynamics. The water production of CBM wells is large in the shallow part of this area. The Wells J25 and J64 in profile A-A' (Fig. 15), which are located near the eastern edge of the study area, continued to drain throughout production, with the highest water production volumes of 156.10 m^3/d and 137.56 m^3/d, respectively. Influenced by this strong groundwater dynamics the average of water production (AWP) and water production per unit dynamic liquid level drop (WPPDLD) are also relatively higher (Fig. 15). Although the initial reservoir pressure is low here, it cannot be effectively reduced during the drainage stage, which led to a retardation of gas desorption. It is noted that gas production is relatively lower in this area, the average of gas production (AGP) and gas production per unit dynamic liquid level drop (GPPDLD) are also relatively lower here (e.g., Well J34 in profile B-B', Well J32 in profile C-C'), even no gas has produced during its drainage procedure in some wells (e.g., Well J25 in profile A-A') (Fig. 18(a)). The active groundwater environment inhibits the production of CBM in this eastern margin area. In the relatively deeper buried area of this slope belt which is located on the east side of the fault zone, the groundwater runoff intensity gradually weakens. The coal seam methane carried by groundwater is reabsorbed and preserved there. The AWP and WPPDLD are relatively lower in this weak runoff zone. Thus, the bottom hole flowing pressure of the well decreases significantly after a continuous drainage process and the gas is desorbed from coal reservoir and transported to wellbore for production. It is noted that gas

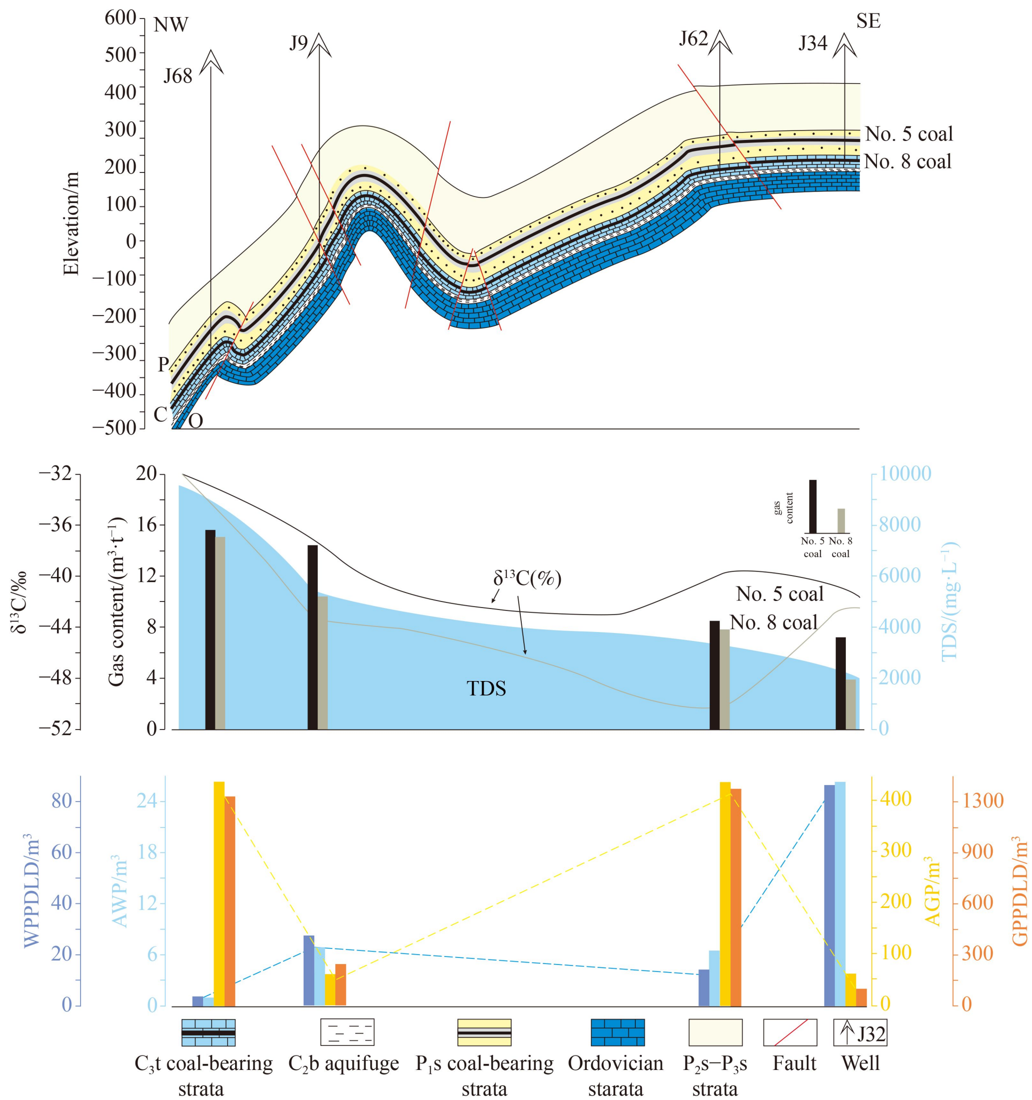

Fig. 16 The characteristic of gas accumulation and production in profile B-B'.

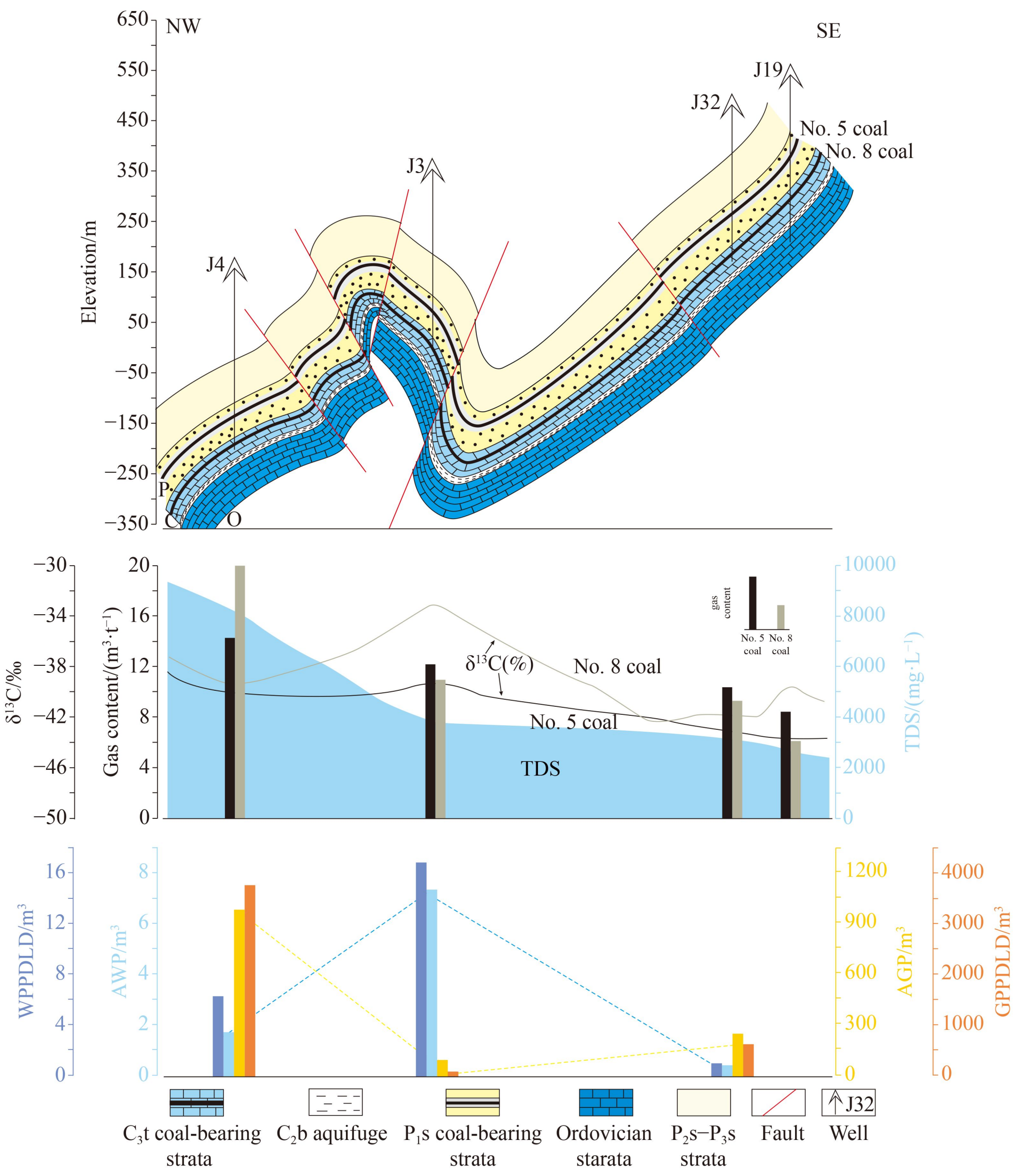

Fig. 17 The characteristic of gas accumulation and production in profile C-C'.

production reaches the peak during the gas-water co-production phase in this slope zone, especially in Wells J35 and J62 (Figs. 16 and 18(b)). The AGP and GPPDLD are relatively higher in well J62 with the highest production rate reaching 1855 m^3/d. However, gas production declines rapidly after the gas-water co-production phase (Fig. 18(b)). It may be caused by damage to coal reservoir as a result of coal dust migration and re-sedimentation during the large water production and rapid gas production.

On the west side of the fault zone, which follows the second model, due to the stagnation of groundwater, the water production parameters (i.e., AWP and WPPDLD) are relatively lower here (Fig. 17). The large buried depth of coal seam leads to a relatively higher initial reservoir pressure. The high ratio of critical pressure to reservoir pressure ensures the gas output easier after drainage and depressurization for a short time. The AWP of Well J4 was only 1.71 m^3/d while the AGP reached 995.89 m^3/d (Figs. 17 and 18(c)). After the gas-water co-production stage, the gas production can be maintained stable at a high value. The high gas content of coal reservoir also ensures the continuous production of CBM.

Generally, the west side of the fault zone is the enrichment and high-yield area for CBM development and CO_2 geological storage in study area.

5 Conclusions

Based on experimental data of the geochemical characteristics of produced fluids (i.e., the produced water and gas) the hydrogeological condition, CBM generation and migration characteristics were analyzed in the Daning-

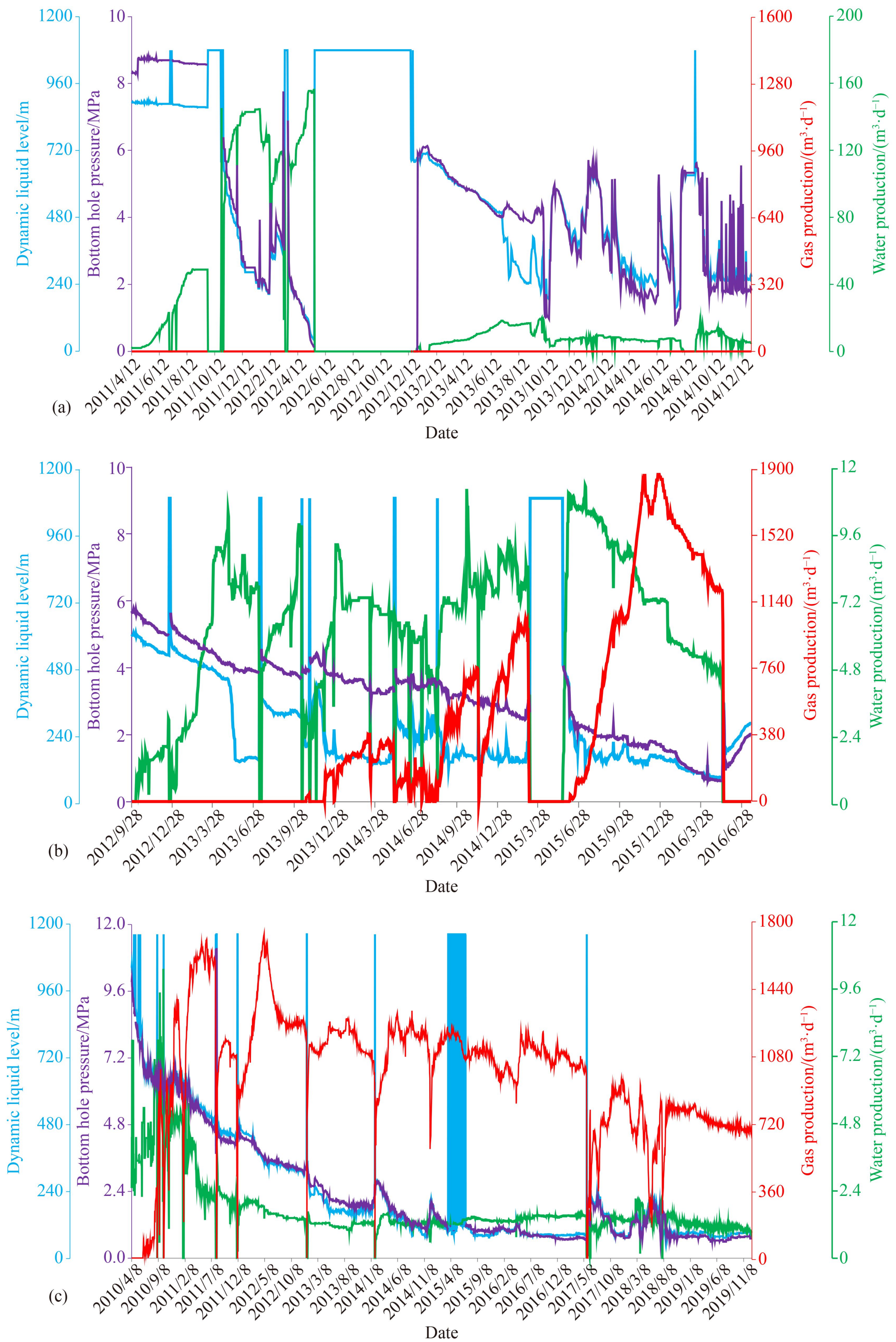

Fig. 18 The characteristics of typical CBM wells production curves. (a) Well J25, (b) Well J62, (c) Well J4.

Jixian block. Then, the geological impacts on gas enrichment and well production were revealed, and a favorite area for CBM development and CO_2 geological storage were proposed.

1) The produced water of CBM wells in the Daning-Jixian block is mainly Na^+, HCO_3^-, Cl^-, and the water

type are $Cl^{-}Na$ and $HCO_3 \cdot Cl^{-}Na$.

2) The Daning-Jixian area can be divided into two hydraulic units (i.e., the recharge-runoff zone and the weak runoff-stagnation zone) while the intensity of runoff gradually decreases and TDS gradually increases westward.

3) The composition of the produced gas is dominated by CH_4, with dry gas characteristics. CBM is mainly origin from thermal gas, secondary biogenic gas supplement only distributed in the eastern edge of the study area. The carbon isotope is significantly less than ideal simulation experiment values due to the hydrodynamic influence.

4) The present-day distribution of the gas content is the result of coupling effects of hydrodynamic, tectonic features and the degree of coal organic matter thermal evolution.

5) Two modes of CBM enrichment appropriate in the Daning-Jixian block. First, CBM is carried by active groundwater, and preserved by resorption in deeply buried footwall areas of reverse faults. Secondly, thermal gas blocked by fault zones is sealed to accumulation in the slope weak runoff-stagnation zone. Different enrichment patterns also caused different gas production characteristics.

6) The west side of the fault zone is the enrichment and high-yield area for CBM development and CO_2 geological storage in the study area.

Acknowledgments This research was funded by the National Natural Science Foundation of China (Grant No. 41902178), the National Science and Technology Major Project (Oil & Gas) (No. 2016ZX05065), the Natural Science Foundation of Shanxi Province, China (No. 20210302123165), the Open Fund of Beijing Key Laboratory of Unconventional Natural Gas Geological Evaluation and Development Engineering, China University of Geosciences (Beijing) (No. 2019BJ02001).

References

Bao Y, Hu Y L, Li D, Sun X Y, Ju Y W (2021). Advance on the genetic mechanism of lighter carbon isotopic composition in coalbed methane. J Xi'an U Sci Tech, 41(6): 1040–1049 (in Chinese)

Chao H Y, Wang Y B (2016). Origin of coalbed methane and its influence in Linfen, southeastern Ordos Basin. J China Coal Soc, 41(7): 1769–1777 (in Chinese)

Chen S D, Tao S, Tian W G, Tang D Z, Zhang B, Liu P C (2021). Hydrogeological control on the accumulation and production of coalbed methane in the Anze Block, southern Qinshui Basin, China. J Petrol Sci Eng, 198: 108138

Chen Y, Ma D M, Fang S Y, Guo C, Yang F, Hou D Z (2019). Enrichment and high-yield models of coalbed methane influenced by geologic structures and hydrologic conditions. J Xi'an U Sci Tech, 39(04): 644–655 (in Chinese)

Dai J X, Qi H F, Song Y, Guan S D (1986). Coal-bed methane composition, carbon isotope types and their genesis and significance in China. Sci China Ser B, 1986(12): 1317–1326 (in Chinese)

Duan Y, Zhao Y, Cao X X, Xu L (2014). Carbon isotope evolution and dynamic characteristics of pyrolysis methane. J China Univ Min Technol, 43(01): 64–71 (in Chinese)

Fu H J, Tang D Z, Pan Z J, Yan D T, Yang S G, Zhuang X G, Li G Q, Chen X, Wang G (2019). A study of hydrogeology and its effect on coalbed methane enrichment in the southern Junggar Basin, China. AAPG Bull, 103(1): 189–213

Hou G C, Zhang M S (2008). Groundwater Exploration in Ordos Basin. Beijing: Geology Press, 317–427 (in Chinese)

Jiang B, Wang J L, Qu Z H, Li C G, Wang L L, Li M, Liu J G (2016). The stress characteristics of the Daning-Jixian area and its influence on the permeability of the coal reservoir. Earth Sci Front, 23(003): 17–23 (in Chinese)

Kaiser W R, Hamilton D S, Scott A R, Tyler R, Finley R J (1994). Geological and hydrological controls on the producibility of coalbed methane. J Geol Soc London, 151(3): 417–420

Kinnon E C P, Golding S D, Boreham C J, Baublys K A, Esterle J S (2010). Stable isotope and water quality analysis of coal bed methane production waters and gases from the Bowen Basin, Australia. Int J Coal Geol, 82(3–4): 219–231

Li W B, Lu S F, Li J Q, Wei Y B, Zhao S X, Zhang P F, Wang Z Y, Li X, Wang J (2022). Research progress on isotopic fractionation in the process of shale gas/coalbed methane migration. Petrol Explor Develop, 49(5): 1069–1084

Li X, Fu X H, Ge Y Y, Chang X X (2016). Research on sequence stratigraphy, hydrogeological units and commingled drainage associated with coalbed methane production: a case study in Zhuzang syncline of Guizhou Province, China. Hydrogeol J, 24(8): 2171–2187

Li Y, Tang D Z, Fang Y, Xu H, Meng Y J (2014). Distribution of stable carbon isotope in coalbed methane from the east margin of Ordos Basin. Sci China Earth Sci, 44(09): 1940–1947

Liu H L, Wang H Y, Zhao Q, Lin Y J, Sang S X, Yong H (2010). Geological characteristics of coalbed methane and controlling factors of accumulation in Tuha Basin. Acta Geol Sin, 84(01): 133–137 (in Chinese)

Liu Q Y, Worden R H, Jin Z J, Liu W H, Li J, Gao B, Zhang D W, Hu A P, Yang C (2014). Thermochemical sulphate reduction (TSR) versus maturation and their effects on hydrogen stable isotopes of very dry alkane gases. Geochim Cosmochim Acta, 137: 208–220

Liu W H, Song Y, Liu Q Y, Qin S F, Wang X F (2003). Evolution of carbon isotope composition in pyrolytic gases generated from coal and its main macerals. Acta Sedimentologica Sin, 2003(1): 183–190 (in Chinese)

Michael F, Anna M, Steven P (2008). Biodegradation of sedimentary organic matter associated with coalbed methane in the Powder River and San Juan Basins, U.S.A. Int J Coal Geol, 76(1–2): 86–97

Moore T A (2012). Coalbed methane: a review. Int J Coal Geol, 101: 36–81

Qi H F (1985). Preliminary comment on the variation of carbon isotopes composition of methane in coal measure gas and seam gas, and its controlling factor. Petrol Geol & Exp, 1985(02): 81–86 (in

Chinese)
Qin S F, Song Y, Tang X Y, Fu G Y (2005). Hydrodynamic influence on carbon isotope of coalbed methane. Nat Gas Ind, 2005(11): 30–32+147 (in Chinese)
Qin S F, Tang X Y, Song Y, Wang H Y (2006). Distribution and fractionation mechanism of stable carbon isotope of coalbed methane. Sci China Earth Sci, 49(12): 1252–1258 (in Chinese)
Scott A R (2002). Hydrogeologic factors affecting gas content distribution in coalbeds. Int J Coal Geol, 50(1–4): 363–387
Sheppard S M F (1986). Characterization and isotopic variations in natural-waters. Rev Mineral, 16(1): 165–183
Sun B, Wang X H, Chen C H, Zhang J D (2004). Distribution characteristic of the coalbed metane at Daning-Jixian region in Ordos Basin. Nat Gas Ind, 24(5): 17–20+144–145 (in Chinese)
Sun Q P, Wang S W (2006). The deposit environment analysis of the coal-bearing strata and its significance to the coalbed methane development in Daning-Jixian region. Nat Gas Geosci, 17(6): 874–879 (in Chinese)
Tao M X, Wang W C, Li Z P, Ma Y Z, Li J, Li X B (2014a). Comprehensive study on genetic pathways and parent materials of secondary biogenic gas in coalbeds. Chin Sci Bull, 59: 992–1001
Tao S, Tang D Z, Xu H, Gao L J, Fang Y (2014b). Factors controlling high-yield coalbed methane vertical wells in the Fanzhuang Block, southern Qinshui Basin. Int J Coal Geol, 134-135: 38–45
Taylor H P (1997). Oxygen and hydrogen isotope relationships in hydrothermal mineral deposits. In: Barnes H L, ed. Geochemistry of Hydrotherm Ore Deposits. New York: John Wiley & Sons, 229–302
Tian W G (2012). CBM enrichment rules of eastern Ordos Basin and controlling mechanism. Dissertation for Doctor’s Degree. Beijing: China University of Geosciences (Beijing) (in Chinese)
Van Voast W A (2003). Geochemical signature of formation waters associated with coalbed methane. AAPG Bull, 87(4): 667–676
Wang B, li j, zhang m (2007). Formation water chemical characteristics of coalbed methane (CBM) reservoir formation. J Oil Gas Tech: 29(5): 66–68+166 (in Chinese)
Wang D (2016). The research of affective facts of production and enrichiment of CBM in Linfen Block. Dissertation for the Doctor’s Degree. China University of Mining &Technology, Beijing (in Chinese)
Wang L L (2014). Evaluation of joint development heterogeneity of coal reservoir based on structural dynamics and its application: an example from Linfen, The eastern margin of the Ordos Basin. Dissertation for the Doctor’s Degree. Xuzhou: China University of Mining and Technology (in Chinese)
Wang L L, Jiang B, Qu Z H (2013). Structural control of gas content in coal seams in eastern margin of Ordos basin. Coal Geo & Explor, 41(1): 14–19 (in Chinese)
Whiticar M J (1999). Carbon and hydrogen isotope systematics of bacterial formation and oxidation of methane. Chem Geol, 161(1–3): 291–314
Yan T T (2016). Geological controls of coalbed methane accumulation evolution in the weibei coalbed methane pilot field. Dissertation for the Doctor’s Degree. Beijing: China University of Geosciences (Beijing) (in Chinese)
Yan X, Li X J, Zhao H, Zhang W, Wang Z B, Mao D L (2015). Research on well interference of coalbed methane wells and its application. Lithol Resour, 27(2): 126–132 (in Chinese)
Yang S F (2003). Comprehensive geological study of coal seam methane in the Daning-Jixian aera of Shanxi Province. Dissertation for the Master’s Degree. Beijing: China University of Geosciences (Beijing) (in Chinese)
Yao Y B, Liu D M, Qiu Y K (2013). Variable gas content, saturation, and accumulation characteristics of Weibei coalbed methane pilot-production field in the southeastern Ordos Basin, China. AAPG Bull, 97(8): 1371–1393
Yao Y B, Liu D M, Yan T T (2014). Geological and hydrogeological controls on the accumulation of coalbed methane in the Weibei field, southeastern Ordos Basin. Int J Coal Geol, 121: 148–159
Ye J P, Wu Q, Wang Z H (2001). Controlled characteristics of hydrogeological conditions on the coalbed methane migration and accumulation. J China Coal Soc, 26(5): 459–462 (in Chinese)
Zhang G W, Dong Y P, Yao A P (2001). Review on the development of studies on the tectonic and orogen process of orogenic belt, and discussing on some new key problems. Northwest Geol, 2001(1): 2–10 (in Chinese)
Zhang J B, Tao M X (2000). Geological significances of coal-bed methane carbon isotopes in coal-bed methane exploration: a case study in Qinshui Basin. Sediment Sin, 2000(4): 611–614 (in Chinese)
Zhang S H, Tang S H, Li Z C, Qiao L H, Men C (2015). The hydrochemical characteristics and ion changes of the coproduced water: taking a Shizhuangnan block, south of the Qingshui Basin as an example. J China Univ Min Technol, 44(2): 292–299 (in Chinese)
Zhang Y, Li S, Tang D Z, Liu J C, Lin W J, Feng X, Ye J C (2022). Geological and engineering controls on the differential productivity of CBM wells in the Linfen block, southeastern Ordos Basin, China: insights from geochemical analysis. J Petrol Sci Eng, 211: 110159
Zhou S D, Yan D T, Tang J G, Pan Z J (2020). Abrupt change of pore system in lacustrine shales at oil- and gas-maturity during catagenesis. Int J Coal Geol, 228: 103557